RESONATORS

PACS numbers: 42.60.Da
DOI: 10.1070/QE2009v039n12ABEH014137

Restrictions in the realisation of multipass unstable resonators

S.Yu. Strakhov

***Abstract*. Main restrictions in the realisation of multipass unstable resonators caused by intracavity losses and large-scale aberrations are considered. The influence of intracavity losses on the laser radiation power and divergence is analysed based on the numerical simulation of an unstable resonator. The efficiency criterion for the unstable multipass resonator is proposed, which is proportional to the radiation brightness and takes into account the influence of the misalignment, thermal deformation and the main parameters of the active medium and resonator on the parameters of laser radiation.**

Keywords: *unstable multipass resonator, intracavity aberrations, resonator optimisation.*

At present the gas flow and supersonic-flow chemical lasers – CO_2 gas-dynamic lasers (GDLs), supersonic chemical oxygen – iodine lasers (COILs), and HF (DF) chemical lasers provide maximum powers and high optical quality of cw radiation. Therefore, such lasers are optimal for many technological applications requiring a high energy density in a processed zone and for solving a number of special problems related to the radiation transport to remote zones and to the force action on objects.

The optimal radiation parameters for such lasers are achieved by using unstable resonators [1]. Such resonators provide a low angular divergence of high-power radiation and can ensure the efficient forced cooling of the output mirror, etc. Concerning the application of unstable resonators in gas flow and chemical lasers, note that all these lasers, despite their different designs and operation principles, have common specific features, namely, the restricted amplification length – the active-medium (AM) size along the radiation propagation direction (in most cases, this is the AM length along a nozzle unit, across the AM flow) and a relatively low small-signal gain, which is, in particular, for CO_2 GDLs and COILs is 0.5 – 1 m^{-1}.

The advantages of unstable resonators are manifested at high enough (more than 1.3 – 1.5) magnification factors. At the same time, these features of lasers under study cannot provide such magnification factors in a single-pass resonator. Unstable resonators can be used in such lasers only in the case of multipass schemes, when radiation propagates several times through the AM between resonator mirrors. As a result, the total amplification length is increased, and it becomes possible to use unstable resonators with relatively high magnification factors [1].

The use of multipass schemes, along with the increase in the magnification factor of the resonator, can also provide the compensation of the inhomogeneity of the small-signal gain in the AM. Such an inhomogeneity downstream is typical for gas flow and chemical lasers.

In particular, the gain in a CO_2 GDL monotonically decreases downstream from the nozzle unit. For this reason, it is reasonable to use in GDLs the multipass schemes with a corner reflector as one of the mirrors, which provide the rotation of the field through 180° after the total transit of radiation in the resonator [2]. The downstream distribution of the small-signal gain in a COIL is described by a parabola with a distinct maximum. In [3], solutions for multipass resonators are presented which provide the efficient compensation for such amplitude inhomogeneity.

Despite the obvious advantages of multipass schemes, which have no real alternative in some cases, it should be noted that they also have disadvantages, which should be taken into account in the development of resonators.

(i) The use of additional mirrors gives rise to additional intracavity losses, resulting in the decrease in the output power.

(ii) A longer length of the resonator and the presence of additional mirrors enhance the resonator sensitivity to misalignments.

(iii) As the length of a telescopic resonator is increased, the radii of curvature of the end mirrors increase, the sag arrows of their reflecting surfaces decrease correspondingly, and the resonator sensitivity to errors in the radii of curvature of mirrors increases. These errors appear during manufacturing of mirrors and due to their thermal deformation during laser operation.

(iv) As the resonator length is increased, the Fresnel number decreases, which leads to the increase in diffraction losses and, hence, to the decrease in the output power and a more inhomogeneous radiation intensity distribution over the aperture (for Fresnel numbers less than 10 – 20).

(v) As the optical path length in the AM increases, the influence of its phase inhomogeneities on the optical quality and divergence of radiation (and its power to a lesser degree) increases.

S.Yu. Strakhov Institute of Laser Instruments and Technologies, D.F. Ustinov 'Voenmekh' Baltic State Technical University, ul. 1-ya Krasnoarmeiskaya 1, 198005 St. Petersburg, Russia; e-mail: strakhov_s@mail.ru

Received 23 April 2009; revision received 13 September 2009
Kvantovaya Elektronika **39** (12) 1153 – 1158 (2009)
Translated by M.N. Sapozhnikov

(vi) The use of multipass schemes reduces the aperture size compared to the case of a single-pass resonator, resulting in the increase in the radiation load on mirrors and increase in the diffraction divergence (in the absence of beam collimation by an external optical system).

Note that these negative factors appear not only when multipass schemes are used but also when the resonator length is increased by increasing the nozzle unit length and the distance between mirrors without increasing the nozzle unit length because of the design features of the laser.

Because of this, the choice of the optical scheme of the resonator, the number of round-trip transits of radiation in the AM and the resonator length is a challenging multiparametric problem, which should be solved taking into account all the positive and negative factors considered above. In this paper, we propose a new approach to the choice of the optimal resonator scheme.

As a goal function for optimisation of an unstable resonator, we can use the quantity X proportional to the far-field radiation intensity:

$$X = P/\theta^2, \quad (1)$$

where P and θ are the laser radiation power and divergence.

Taking into account the above-mentioned factors affecting the resonator parameters, the criterion X can be written as

$$X = \frac{(1-\bar{P}_{\rm a})(1-\bar{P}_{\rm r})P_0}{\beta^2\theta^2}, \quad (2)$$

where P_0 is the radiation power in the absence of intracavity aberrations; $\bar{P}_{\rm a} = (\Delta P_0)_{\rm a}/P_0$ is the relative decrease in the output power caused by the misalignment of mirrors; $\bar{P}_{\rm r} = (\Delta P_0)_{\rm r}/P_0$ is the relative decrease in the output power caused by variations in the radius of curvature of mirrors due to technological errors and thermal deformations during laser operation; $(\Delta P_0)_{\rm a}$ and $(\Delta P_0)_{\rm r}$ are the absolute decrease in the output power caused by misalignment and variations in the radius of curvature, respectively; β is the optical quality factor of the AM, which is the ratio of the laser radiation divergence in the presence of phase inhomogeneities in the AM to that divergence in the ideal AM.

The value of β depends considerably on the inhomogeneity of the refractive index of the AM and the optical path length propagated by radiation in the resonator. The optical quality of the AM can be characterised by the Strehl (Sh) number after one transit of radiation in the AM. The value of β is related to the Strehl number by the expression

$$\beta = {\rm Sh}^{-0.5}.$$

The Strehl number in turn can be determined quite accurately from the dispersion D_φ of the wave-front phase of laser radiation: ${\rm Sh} \approx \exp(-D_\varphi)$. The level of inhomogeneities of the refractive index and, hence, the value of β is proportional to the average density of the AM. In particular, the influence of β in COILs is negligible compared to other factors ($\beta = 1.02 - 1.05$ for ${\rm Sh} = 0.98 - 0.95$). The value of β also strongly depends on the specific distribution of the refractive index of the AM, which is determined by the method of mixing its components, the design of the nozzle unit and resonator chamber, etc. The influence of optical inhomogeneities of the AM on the resonator operation has been studied in many papers, in particular in [1, 4].

The divergence angle in (2) can be represented with a certain precision degree as a superposition of three independent components: the diffraction component, the component related to the resonator misalignment, and the component caused by deviations of the radii of curvature of mirrors from the rated value, which appear due to errors in the manufacturing of mirrors and due to thermal deformations:

$$\theta^2 = \left[\left(\frac{\theta_{\rm r}}{\theta_0}\right)^2 + \left(\frac{\theta_{\rm a}}{\theta_0}\right)^2 + 1\right]\theta_0^2. \quad (3)$$

Here, $\theta_0 = 2(\lambda/d)M/(M-1)$ is the diffraction divergence angle (for an unstable confocal resonator with the emitting aperture diameter d and the magnification factor M); $\theta_{\rm a}/\theta_0$ and $\theta_{\rm r}/\theta_0$ is the increase in the divergence angle with respect to the diffraction angle, which is caused by the resonator misalignment and deformation of its mirrors, respectively.

The influence of the optical inhomogeneities on the angular divergence could be taken into account by adding another component to (3); however, here we use for this purpose the optical quality factor β [see (2)], as in [5].

The influence of intracavity aberrations caused by the misalignment and thermal deformation of mirrors (errors in the manufacturing of mirrors are neglected here) on the radiation power and divergence depending on the resonator parameters (the magnification factor M and the Fresnel number $N_{\rm F}$) was studied by numerical simulations by the method used in [6]. The resonator was calculated in the diffraction approximation by the spectral method by using the fast Fourier transform algorithm. For this purpose, the three-dimensional calculation region of the unstable resonator was divided into separate segments restricted by amplitude – phase screens along the radiation propagation direction. All calculations were performed for a square 512×512 network, the central region of the network of size 256×256 nodes being inscribed to the AM aperture, while the remaining nodes (by 128 nodes on each side) represented the 'protective zone'. The active medium was divided into five identical segments. Empty regions between each of the mirrors and the corresponding AM boundary represented two other segments. This configuration of the calculation region provided the sufficient calculation accuracy for unstable resonator schemes under study.

The complex field amplitude of a light wave for each ith screen was multiplied by the amplitude – phase factor A_i characterising the integrated gain and aberration properties of the AM inside a segment:

$$u_i(x,y,z) = u(x,y,z)A_i(x,y),$$

$$A_i(x,y) = \exp[{\rm i}\varphi(x,y)]\exp(gL_i/2),$$

where $\varphi(x,y)$ is the change in the radiation phase after the propagation of radiation through the AM segment in front of the ith screen (we assume here that the medium is ideal and $\varphi(x,y) = {\rm const}$); g is the AM gain; L_i is the length of the segment in front of the ith screen in the radiation propagation direction.

In this paper, we used the simplest AM gain model in which the gain at each point is described by the expression

$$g = \frac{g_0}{1 + I/I_s},$$

where g_0 is the small-signal gain; I_s is the saturation intensity; and I is the current radiation intensity.

We studied a confocal unstable resonator of the positive branch, as the most popular one. The influence a large-scale phase inhomogeneity of the lens type (thermal deformation) or an optical wedge (misalignment) located on a concave mirror of a two-mirror (single-pass) unstable resonator was numerically stimulated. Simulations were performed for the magnification factor M and Fresnel number $N_F = d^2/(4\lambda L)$, where L is the resonator length. The parameters characterising the level of large-scale inhomogeneities were varied. They included the relative misalignment angle of the resonator $\Delta\bar{\alpha} = \alpha d/\lambda$, where α is the absolute misalignment of a mirror (the value of $\Delta\bar{\alpha}$ is proportional to the phase change on the mirror caused by its misalignment) and the relative value $\bar{\omega} = \omega/\lambda$ of the mirror deformation, which is proportional to the wave-front distortion, where ω is the absolute deformation of the mirror (the value of $\bar{\omega}$ is proportional to the sag arrow of the mirror with respect to the rate surface expressed in wavelengths).

Before the calculation of the radiation energy transfer to the far-field region for determining the radiation pattern parameters and the radiation divergence angle from the wave front, we separated large-scale phase aberrations (spherical and linear) and performed their numerical 'compensation', i.e. the residual (after the separation of a sphere or a wedge) wave front was considered, as, for example, in [7]. This operation is performed because in practice these components are separated by simple refocusing (for the spherical component) or the tilt of the radiation propagation axis (for the linear phase component).

The simulations gave the calculated dependences of $\bar{P}_a$, θ/θ_0, and $\bar{P}_r$ presented in Figs 1–3. The numerical simulations showed that the spherical phase aberration caused by the thermal deformation of mirrors reduces the output power and gives rise to a large-scale spherical component in the wave-front structure of laser radiation. After the compensation of this component, the radiation wave front proves to be close to the wave front produced by a similar resonator in the absence of mirror aberrations. Therefore, for the residual (after the separation of the spherical component) wave front, we have $\theta_r/\theta_0 = 0$.

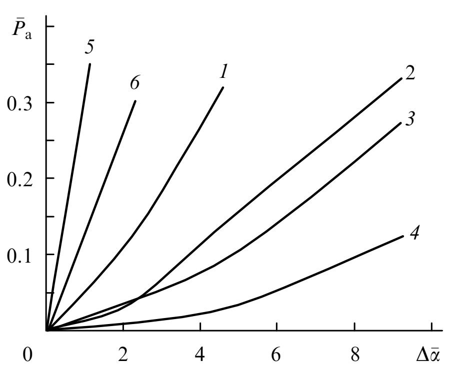

Figure 1. Dependences of the relative decrease in the output power $\bar{P}_a$ on the relative misalignment $\Delta\bar{\alpha}$ of the concave mirror of the unstable resonator for $M = 1.5$, $N_F = 79$ (*1*); $M = 2.0$, $N_F = 9$ (*2*); $M = 1.5$, $N_F = 314$ (*3*); $M = 2.0$, $N_F = 314$ (*4*); $M = 1.5$, $N_F = 19$ (*5*); $M = 1.3$, $N_F = 78$ (*6*).

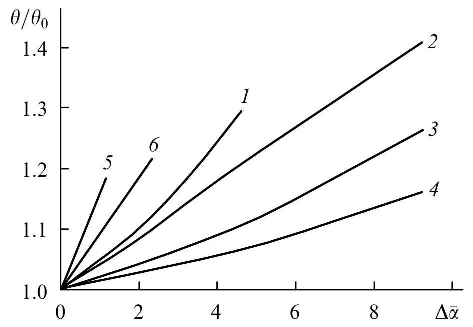

Figure 2. Dependences of the relative divergence angle θ/θ_0 on the relative misalignment $\Delta\bar{\alpha}$ of the concave mirror of the unstable resonator for $M = 1.5$, $N_F = 79$ (*1*); $M = 2.0$, $N_F = 79$ (*2*); $M = 1.5$, $N_F = 314$ (*3*); $M = 2.0$, $N_F = 314$ (*4*); $M = 1.5$, $N_F = 19$ (*5*); $M = 1.3$, $N_F = 78$ (*6*).

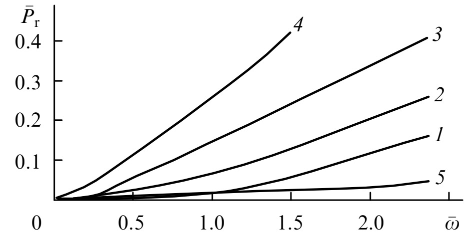

Figure 3. Dependences of the relative decrease in the output power $\bar{P}_r$ on the relative misalignment $\bar{\omega}$ of the concave mirror of the unstable resonator for $M = 2.0$, $N_F = 79$ (*1*); $M = 1.5$, $N_F = 79$ (*2*); $M = 1.3$, $N_F = 79$ (*3*); $M = 1.5$, $N_F = 19$ (*4*); $M = 1.5$, $N_F = 314$ (*5*).

Depending on the resonator design and the method of its alignment, the real values of α achieved in practice can be considerably different. In particular, in the case of manual alignment and visual control of the alignment, the values $\alpha = 10 - 20''$ can be achieved, while in the case of automated alignment by using piezoceramic drives for mirrors and a CCD array to control the alignment process, the value $\alpha = 5 - 10''$ can be achieved. In addition, it should be noted that laser mirrors can be misaligned during laser operation due to vibrations, force loads on the bearing elements of the resonator, etc., which deteriorates the accuracy of the angular position α of mirrors achieved in the initial alignment.

The characteristic thermal deformations ω of mirrors during laser operation can be determined from thermal calculations of mirrors by the methods presented in [8]. In particular, we can use the relation

$$\omega = \frac{\xi_{ab} I_m b^2}{2} \frac{\gamma_T}{\lambda_T}, \tag{4}$$

where I_m is the radiation intensity incident on mirrors; ξ_{ab} is the absorption coefficient of the mirror; b is the laser beam radius; γ_T is the linear temperature expansion coefficient; λ_T is the heat conduction. Depending on the laser type, mirror parameters, and radiation power, the sag arrow can vary in a broad range from 0.1 to 10 μm.

All the presented data, as mentioned above, were obtained by numerical simulations of large-scale inhomogeneities located on the concave mirror of the resonator. The results can be generalised for multimirror resonators by assuming that the large-scale first- and second-order phase aberrations introduced by each mirror are independent. In this case, the total intracavity aberration can be written in the form

$$\bar{\varpi}_{\Sigma}^2 = \sum_{i=1}^{N} \bar{\varpi}_i^2 = N\bar{\varpi}_i^2,$$
$$\Delta\bar{\alpha}_{\Sigma}^2 = \sum_{i=1}^{N} \Delta\bar{\alpha}_i^2 = N\Delta\bar{\alpha}_i^2, \qquad (5)$$

where N is the total number of reflections from mirrors during a round-trip transit of radiation in the resonator; $\Delta\bar{\alpha}_i$ and $\bar{\varpi}_i$ are the relative misalignment and deformation, respectively, introduced by each mirror. Similar dependences can be also written for the absolute values of misalignment angles α and thermal deformations ω.

The output power of a laser by neglecting intracavity aberrations can be estimated from the expression [9]

$$P_0 = \frac{I_s tF}{2}\left[\frac{2g_0 L_{\rm am} + \ln(1-t-\chi)}{-\ln(1-t-\chi)}\right], \qquad (6)$$

where F is the area of the emitting aperture (for a stable resonator); t is the transmission coefficient of the output mirror; $L_{\rm am}$ is the AM length; and χ is intracavity losses not related to aberrations.

The transmission coefficient of an unstable resonator is related to the magnification factor by the expression $t = 1 - 1/M^2$. In this case, F is equal to the cross-sectional area of a laser beam incident on the output mirror.

Intracavity power losses, not related to aberrations, are determined by inactive absorption in the AM, which can be neglected for gas lasers, diffraction losses, and losses on mirrors. The diffraction losses are determined by the Fresnel number $N_{\rm F}$; for $N_{\rm F} > 20 - 50$, diffraction losses become negligible. The power loss on mirrors is equal to the product of the number N of reflections from mirrors during a round-trip transit of radiation in the resonator by losses χ_0 on one mirror.

Taking (3), (5), and (6) into account, expression (2) can be written in the form

$$X = \frac{[1-\bar{P}_{\rm a}(N_{\rm F}, M, \Delta\bar{\alpha}_{\Sigma})][1-\bar{P}_{\rm r}(N_{\rm F}, M, \bar{\varpi}_{\Sigma})]}{\beta^2\theta_0^2[\theta(N_{\rm F}, M, \Delta\bar{\alpha}_{\Sigma})/\theta_0]^2} \times \frac{I_s(1-1/M^2)F}{2}\left\{\frac{2g_0L_{\rm am} + \ln[1/M^2 - \chi(N, N_{\rm F})]}{-\ln[1/M^2 - \chi(N, N_{\rm F})]}\right\}$$
$$\approx \frac{[1-\bar{P}_{\rm a}(N_{\rm F}, M, \Delta\bar{\alpha}_{\Sigma})][1-\bar{P}_{\rm r}(N_{\rm F}, M, \bar{\varpi}_{\Sigma})]}{\beta^2[(2\lambda/d)(M/(M-1))]^2[\theta(N_{\rm F}, M, \Delta\bar{\alpha}_{\Sigma})/\theta_0]^2} \times \frac{I_s(1-1/M^2)F}{2}\left[\frac{2g_0L_{\rm am} + \ln(1/M^2 - \chi_0 N)}{-\ln(1/M^2 - \chi_0 N)}\right]. \qquad (7)$$

As an example of using (7) for optimisation of multipass unstable resonators, we consider the unstable resonator with the following parameters: the AM of size 0.12×0.12 m, the AM length is $L_{\rm am} = 1$ m, the distance between mirror plate is 1.7 m, the small-signal gain is $g_0 = 0.5$ m^{-1}, the saturation intensity is 2 kW cm^{-2}, the radiation wavelength is $\lambda = 10.6$ μm; and the optical quality of the AM is assumed ideal ($\beta = 1$).

The thermal deformation of the mirror, determined from expression (4) for the radiation power 50 kW, $b = 0.06$ m. $\xi_{\rm ab} = 0.015$, $\gamma_T = 16.7 \times 10^{-6}$ K^{-1} and $\lambda_T = 400$ W m$^{-1}\times$ K^{-1} (copper mirrors), was $\omega = 5.6$ μm for one mirror, or $\bar{\varpi} = 0.53$.

We considered single-pass, double-pass, three-pass, and four-pass unstable resonators. The schemes and main parameters of these resonators are presented in Table 1.

The size d of the emitting aperture in (7) was assumed the same for all resonators, and it was also assumed that the

Table 1. Main parameters of unstable resonators.

Unstable resonator type and scheme	Aperture size/m	$L_{\rm am}(L)$/m	$N_{\rm F}$	N	χ (for $\chi_0 = 0.015$)	$\Delta\bar{\alpha}_i$ (for $\alpha = 20''$)	$\Delta\bar{\alpha}_{\Sigma}$	$\bar{\varpi}_{\Sigma}$ (for $\omega = 5.6$ μm)	$(\Delta P)_{\rm a}/P_0$ (for $M = 1.5$)	$(\Delta P)_{\rm r}/P_0$ (for $M = 1.5$)	θ/θ_0 (for $M = 1.5$)
Single-pass 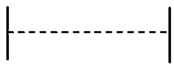	0.12×0.12	1(1.7)	200	2	0.03	1.10	1.56	0.71	0.02	0.03	1.04
Double-pass (squared) 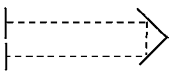	0.12×0.06	2(3.4)	56	6	0.09	0.83	2.03	1.22	0.16	0.15	1.15
Three-pass (Z-shaped) 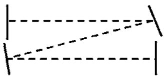	0.12×0.06	2.5(5)	38	6	0.09	0.83	2.03	1.22	0.22	0.15	1.23
Four-pass 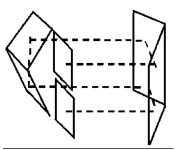	0.06×0.06	4(6.8)	12	14	0.21	0.55	2.06	1.87	0.45	0.55	1.45

output laser beam was collimated to the diameter of the principal mirror of the collimating system ($d = 1$ m in calculations).

Figures 4 and 5 show the dependences of the radiation power and criterion X on M. The criterion was determined from expression (7) for ideal and real unstable resonators. The ideal resonator has no aberrations, and mirror losses in this resonator are 0.01. The real resonator was simulated taking into account large-scale intracavity aberrations caused by mirror misalignments and thermal deformations, as well as reflection losses depending on the number of mirrors used in the resonator. We assumed in calculations that misalignment errors are $20''$ for each mirror and the absolute thermal deformation of each mirror, as mentioned above, is 5.6 μm.

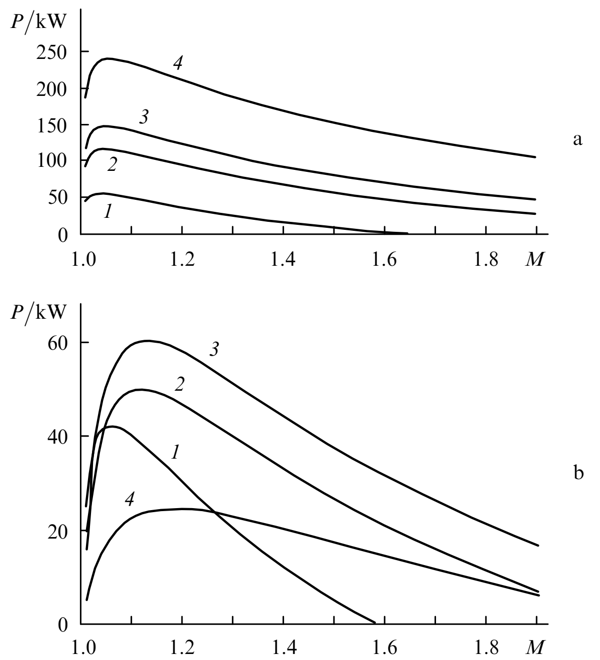

Figure 4. Dependences of the output power on the magnification factor M for single-pass (*1*), double-pass (*2*), three-pass (*3*), and four-pass (*4*) resonators by neglecting intracavity aberrations for total losses $\chi = 0.01$ (a) and taking into account intracavity aberrations and real losses according to Table 1 (b).

It follows from Figs 4 and 5 that in the case of the ideal resonator simulated without intracavity aberrations and considerable losses, the output power and radiation divergence increase quite predictably, i.e. multipass resonators prove to be more efficient.

The situation changes when intracavity losses and aberrations are taken into account. One can see from Figs 4 and 5 that the resonator efficiency, determined by the output power and criterion X, increases only if the number of transits of radiation in the resonator does not exceed three. The efficiency of the four-pass resonator expressed by the criterion X is lower than that of the three- and double-pass resonator, whereas the efficiency of the former resonator with respect to the output power is lower than that of all other resonators under study. This is explained by a drastic increase in intracavity losses and the enhancement of the influence of phase aberrations on radiation parameters in the four-pass resonator with a large

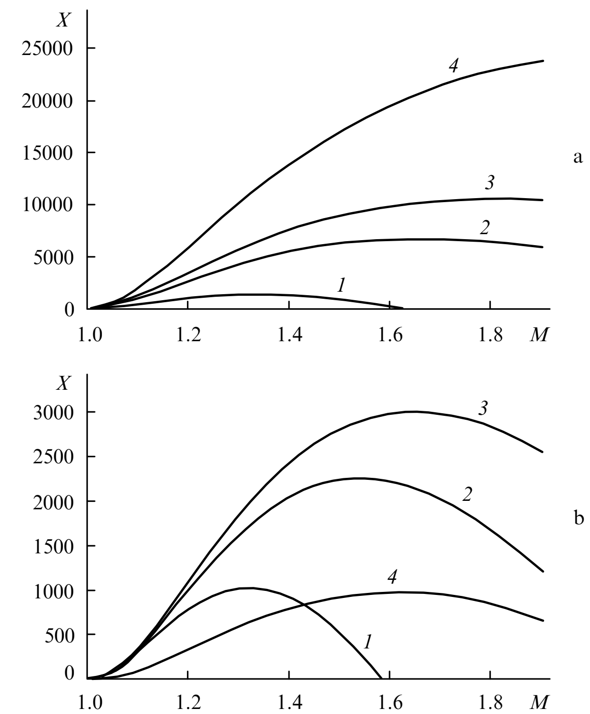

Figure 5. Dependences of the criterion on the magnification factor for single-pass (*1*), double-pass (*2*), three-pass (*3*), and four-pass (*4*) resonators by neglecting intracavity aberrations for total losses $\chi = 0.01$ (a) and taking into account intracavity aberrations and real losses according to Table 1 (b).

number of reflections from mirrors during the propagation of radiation in the resonator (see Table 1).

This situation is aggravated by the fact that the effective aperture of the four-pass resonator under real conditions is even smaller (which is related to unavoidable gaps between mounting planes of mirrors), and hence, the filling of the AM by radiation will be smaller and the output power will decrease. In addition, the four-pass resonator has other, less formalised disadvantages, such as a more complicated alignment procedure, a complicated design, a smaller aperture diameter requiring a stronger collimation of the laser beam to match the diameter of the principal mirror of the collimating system, etc.

Thus, the increase in the number of passages of radiation (more then three) in the considered example is not reasonable from the point of view of the resonator efficiency. The optimal number of transits of radiation in the resonator depends, of course, on the real conditions of the problem and should be determined separately in each specific case. However, the method itself proposed here is quite universal; it can be also supplemented by the consideration of optical inhomogeneities of the AM with the help of the optical quality factor β, if these inhomogeneities are reliably known. The optimisation method considered in the paper was verified, in particular, in the design of multipass resonators of the 100-kW GDL [2] and 10-kW COIL [10].

In conclusion, we formulate the main results of the study.

(i) The design of multipass unstable resonators is restricted by a number of objective factors preventing the increase in their efficiency by increasing the number of transits of radiation in the resonator, thereby increasing the AM along the resonator axis.

(ii) Restrictions in the realisation of multipass resonators are caused first of all by increasing mirror losses and a stronger dependence of the output radiation on large-scale intracavity inhomogeneities caused by mirror misalignments and thermal deformations during laser operation.

(iii) Multipass resonators can be optimised by using the complex criterion (7), which takes into account the dependence of laser radiation of mirror misalignments, thermal deformations and basic parameters of the AM and resonator.

References

1. Anan'ev Yu.A. *Opticheskie rezonatory i problema raskhodimosti lazernogo izlucheniya* (Optical Resonators and Laser Radiation Divergence) (Moscow: Nauka,1979).
2. Boreisho A.S., Leonov A.F., Strakhov S.Yu., Trilis A.V. *Kvantovaya Elektron.*, **33**, 177 (2003) [*Quantum Electron.*, **33**, 177 (2003)].
3. Savin A.V., Strakhov S.Yu., Druzhinin S.L. *Kvantovaya Elektron.*, **36**, 867 (2006) [*Quantum Electron.*, **36**, 867 (2006)].
4. Orlova I.B. *High Technol.*, **45**, 55 (1997).
5. Dauty J. *Aerokosm. Tekh.*, (2), 53 (1990).
6. Sigman A.E., Sziklas E.A. *Appl. Opt.*, **14**, 1874 (1975).
7. Lobachev V.V., Strakhov S.Yu. *Opt. Zh.*, **67**, 66 (2000).
8. Kharitonov V.V. *Teplofizicheskii raschet lazernykh zerkal* (Thermal Calculations of Laser Mirrors) (Moscow: Izd. MIFI. 1985).
9. Losev S.A. *Gazodinamicheskie lazery* (Gas-dynamic Lasers) (Moscow: Nauka, 1977).
10. Boreisho A.S., Mal'kov V.M., Savin A.V., Vasil'ev D.N., Evdokimov I.M., Trilis A.V., Strakhov S.Yu. *Kvantovaya Elektron.*, **33**, 307 (2003) [*Quantum Electron.*, **33**, 307 (2003)].